Journal of Catalysis 269 (2010) 340–350

Contents lists available at ScienceDirect

Journal of Catalysis

journal homepage: www.elsevier.com/locate/jcat

Catalytic methylation of phenol on MgO – Surface chemistry and mechanism

Fabrizio Cavani [a,b,*], Luca Maselli [a,b], Sauro Passeri [a,b], Johannes A. Lercher [c,*]

[a] Dipartimento di Chimica Industriale e dei Materiali, ALMA MATER STUDIORUM Università di Bologna, Viale Risorgimento 4, 40136 Bologna, Italy
[b] INSTM, Research Unit of Bologna, Italy
[c] Technische Universität München, Department Chemie, Lichtenbergstr. 4, D-85748 Garching, Germany

ARTICLE INFO

Article history:
Received 9 September 2009
Revised 16 November 2009
Accepted 18 November 2009
Available online 29 December 2009

Keywords:
Basic catalysis
Phenol methylation
Reaction mechanism
Electrophilic substitution
Magnesium oxide

ABSTRACT

Reactions of phenol and methanol catalyzed by MgO have been explored by kinetic measurements and *in situ* IR spectroscopy combined with computational studies of sorbed molecules. On MgO, methanol partly transforms to formaldehyde above 250 °C. Adsorbed phenol forms phenolate species, and the energetically preferred mode of adsorption leads to an almost orthogonal orientation of the aromatic ring with respect to the catalyst surface. All molecules involved adsorb preferably at the corner sites of MgO (three-co-ordinated Mg atoms). The main reaction products are anisole and *o*-cresol, the latter dominating above 300 °C. At very low conversions, salicylic aldehyde is observed as primary reaction product, being rapidly transformed to *o*-cresol. It is only observed during the initial accumulation of adsorbed species on the catalyst surface, but not under steady-state conditions on a fully covered catalyst surface. Therefore, *o*-cresol formation starts with the reaction between phenol and formaldehyde to salicylic alcohol, which in turn is rapidly transformed to salicylic aldehyde and subsequently to *o*-cresol. Salicylic aldehyde may also form via the bimolecular disproportionation of salicylic alcohol to *o*-cresol and aldehyde. The parallel reaction to *o*-cresol, not involving the formation of salicylic aldehyde as intermediate, proceeds via the reduction of salicylic alcohol to *o*-cresol by formaldehyde. The identified mechanism may open new synthetic approaches for the production of functionalized phenol derivatives and, even more importantly, for the defunctionalization of substituted phenols potentially available at large scale from deconstructed lignin.

1. Introduction

The methylation of phenol and phenol derivatives has a high industrial relevance. 2,6-Xylenol is, for example, the monomer for the production of poly-(2,6-dimethyl)phenylene oxide resin, 2-methylphenol (*o*-cresol) is the monomer for the synthesis of epoxycresol paints, 2,5-dimethylphenol is the intermediate for the synthesis of dyes, antiseptics, and antioxidants, and 2,3,6-trimethylphenol is the starting compound for the synthesis of vitamin E. The products of ortho-methylation of phenol or anisole and of diphenols, such as guaiacol, are intermediates in the production of skin-protecting agents and food additives.

The ring methylation of phenol to *o*-cresol is industrially carried out with methanol as alkylating agent over basic catalysts [1–6]. Typical catalysts are (supported) alkali and alkaline-earth metal oxides [7–10], (mixed) transition metal oxides [11–23], and combination of both [24–33]. These catalysts show very high regioselectivity in the methylation of the aromatic ring as well as high chemo-selectivity with only minor amounts reacting via oxofunctionalization.

The major problem of the industrial process of phenol methylation is the decomposition of methanol and, consequently, a large excess of methanol has to be fed usually in order to reach an acceptable per-pass conversion of phenol [34]. In this context it is surprising that the potential role of methanol surface chemistry and eventual decomposition during the alkylation of phenols is hardly addressed [12,24,35]. It should be noted here that usually the alkylation of the aromatic ring with methanol is catalyzed by acids [36,37] and that bases catalyze the alkylation of side chains substituted to the aromatic ring (e.g., side-chain alkylation of toluene). For the latter reaction, the dehydrogenation of methanol to formaldehyde was shown to be a prerequisite [38–40].

Acid catalysis transforms methanol into an electrophilic species (alkoxy group or a methyl carbenium ion) able to alkylate both the methanol oxygen and the carbon of the aromatic ring [41,42]. Bases, in contrast, catalyze dehydrogenation of methanol to formaldehyde that in turn primarily alkylates the carbon atoms of the aromatic ring [41,42]. The regioselective preference of the alkylation is related to the negative charge at the carbon atom of the aromatic ring. In the case of phenol it is the ortho and para positions relative to the O–H group. In competing reaction pathways,

* Corresponding authors. Fax: +39 051 209 3680.
E-mail addresses: fabrizio.cavani@unibo.it (F. Cavani), johannes.lercher@ch.tum.de (J.A. Lercher).

0021-9517/$ - see front matter © 2009 Elsevier Inc. All rights reserved.
doi:10.1016/j.jcat.2009.11.019

also methyl formate decomposition products such as CO, CO_2, CH_4, and H_2 are formed from formaldehyde. These first experiments indicate that the main role of the catalyst is the formation of formaldehyde, which preferentially occurs with strongly basic catalysts. The further catalytic chemistry seems to depend then on the availability of formaldehyde under reaction conditions. If this surface chemistry is indeed prevailing, the base-catalyzed route to alkylate aromatic rings would be a highly robust chemo-selective alkylation in the presence of strongly nucleophilic groups.

In the present work, we explore the catalysis with MgO as typical (albeit not most active) catalyst with the aim of establishing the detailed mechanism of catalysis alkylation of aromatic compounds with nucleophilic functionalization. Phenol is used as substrate for conversion, as its simplicity offers a better route for probing the surface chemical species by a combination of *in situ* vibrational spectroscopy and theoretical calculations. The measurements and calculations allow us to postulate and test the kinetic sequence of elementary steps and to lead to clear design parameters for the selective alkylation of functionalized aromatic compounds.

2. Experimental

The employed catalysts were a commercial MgO, supplied by Acros Organics, and a self-synthesized MgO, having specific surface areas of 12 and 68 m^2/g, respectively [42].

Catalytic tests were carried out by vaporization of a methanol/phenol liquid mixture (methanol/phenol molar ratio 10/1; liquid flow 0.0061 ml/min; phenol supplied by Sigma Aldrich, 99+% purity; methanol supplied by Carlo Erba Reagenti, purity 99%) in a N_2 stream (gas flow 20 N ml/min). The liquid mixture was fed by means of a syringe pump (Precidor Type 5003, Infors HT). The composition of the feed gas was the following (molar fractions): methanol 0.108, phenol 0.011, and nitrogen 0.881. The residence time was 2.7 s (in experiments varying the temperature), or was varied in order to obtain very low phenol conversions (<0.5%), at 300 °C. In the latter case, experiments were carried out at contact time lower than 0.2 s, achieved by varying the liquid stream from 0.037 to 0.003 ml/min, and correspondingly the N_2 stream in order to keep constant the reagent/nitrogen molar ratio; each test was carried out by loading 0.2 g of fresh catalyst. Total pressure was one bar. In tests made by feeding salicylic alcohol (Sigma Aldrich, purity 99.9%) and water, the composition of the feed gas was (molar fractions): salicylic alcohol 0.004, water 0.437, and balance nitrogen. In tests made by feeding salicylic alcohol or salicylic aldehyde in formalin (20.6 wt.% formaldehyde in water, containing 0.4% methanol), the composition of the feed gas was (molar fractions): salicylic alcohol 0.005 or salicylic aldehyde 0.0005, formaldehyde 0.054, water 0.354, methanol 0.002, and balance nitrogen.

The gas/vapor stream was fed into a tubular glass reactor (length 300 mm, inner diameter 19 mm) containing either 1 cm^3 of catalyst (catalyst weight 0.85 g, experiments with varying temperature) or variable amounts of catalyst (experiments with varying residence time) shaped in 250–500 μm particles. Catalyst particles were prepared by pressing the calcined powder to obtain pellets that were then broken into smaller granules. During catalytic experiments, the reactor exit stream was condensed in 25 ml of HPLC-grade acetone for 1 h maintained at 6 °C. Products condensed in acetone were analyzed by gas chromatography, using a GC6000 Carlo Erba instrument equipped with a FID and a HP-5 column. The GC oven temperature was programed from 50 to 250 °C, with a heating rate of 10 °C/min. Non-condensable gases (CO, CO_2, H_2, and CH_4) were analyzed by sampling the gaseous stream with a syringe at the reactor exit, before condensation in acetone, and by injecting the sample in a GC4300 Carlo Erba gas chromatograph equipped with a TCD and a Carbosieve SII column. The GC oven temperature was programed from 55 to 220 °C with a heating rate of 10 °C/min.

Yields are expressed as follows:

$$\text{Yield to products of phenol methylation} = \frac{\dot{n}^{out}_{product}}{\dot{n}^{in}_{phenol}},$$

where "product" stands for *o*-cresol, 2,6-xylenol, anisole, and salicylic aldehyde.

Conversion is expressed as follows:

$$\text{Conversion of phenol}: \frac{\dot{n}^{in}_{phenol} - \dot{n}^{out}_{phenol}}{\dot{n}^{in}_{phenol}}.$$

Selectivity to a compound is expressed as the ratio between the corresponding yield and the reactant conversion.

The computational study was carried out on a model $Mg_{12}O_{12}$ cluster. The cluster geometry was taken from Ref. [43] where the Mg–O distance is 2.10850 Å. Density functional theory (DFT) calculation was performed using the B3LYP hybrid density functional, and the 6-31G(d,p) basis set was used. The geometry of all adsorbed molecules was fully optimized, but the substrate cluster was not relaxed in the optimization process in agreement with an experimental study that demonstrated a poor relaxation in this oxide [44]. In order to improve the visual comparison between experimental and calculated IR spectra, wavenumbers have been scaled by a factor of 0.9613 [45]. The adsorption energies were computed as the difference between the energy of MgO/molecule system and the sum of the energies of the separated fragments, $E_{ads} = E_{(MgO-MOL)} - E_{MgO} - E_{MOL}$. Correction for the zero point contribution and, when needed, basis set superimposition error (BSSE), by the counterpoise method, were applied. All calculations were carried out using Gaussian 03 program package [46]. Optimized structures are visualized using GaussView program [47]. Calculations have been carried out on IBM SP5/512 supercomputer at CINECA.

The IR spectra after adsorption of reactant and potential product molecules (phenol, methanol, *o*-cresol, salicylic alcohol, and salicylic aldehyde) were recorded using a Perkin Elmer 1750 FT-IR Spectrometer equipped with a DTGS detector at a resolution of 2 cm^{-1}. MgO samples were pressed into self-supported wafer and activated *in situ* in the IR cell at 450 °C under vacuum (<10^{-7} mbar) for 2 h. Before measuring the IR spectra, the activated sample was contacted with 2–4 mbar of the adsorbent either at 250 °C, or at increasing temperatures from ambient to 550 °C. For recording spectra, 25 scans were co-added. The IR spectra reported are displayed as difference absorbance spectra of the sample with and without the absorbed molecule.

The *in situ* IR spectra were recorded using a Bruker IFS 88 FT-IR spectrometer equipped with an *in situ* flow cell, which was described previously [48,49]. For recording spectra, 60 scans (1 scan/s) were co-added at a resolution of 4 cm^{-1}. Either methanol or a mixture of methanol and phenol (molar ratio 10/1) was vaporized in a He stream (20 mol% of organic components in the He stream) and fed into the cell. Spectra are reported after subtraction of the spectrum of MgO.

3. Results

3.1. Catalytic phenol methylation

The catalytic gas-phase methylation of phenol with methanol over low-surface-area MgO yields *o*-cresol and 2,6-xylenol as the principal reaction products (see Fig. S1 of Supplementary material)

[41,42]. At low temperatures, i.e., below 300 °C, also anisole formed (selectivity less than 25%), but its selectivity decreased and disappeared above 350 °C. The variation in yield at 300 °C as a function of the conversion of phenol is shown in Fig. 1. These tests were carried out by varying the gas residence time, under conditions aimed at obtaining very low phenol conversion (less than 0.5%), in order to detect the formation of the truly primary reaction products.

The primary products were salicylic aldehyde and anisole; however, also a direct contribution for *o*-cresol cannot be excluded indicating that three parallel reaction pathways exist. With increasing conversion, salicylic aldehyde was reduced to *o*-cresol. Thus, *o*-cresol is produced *via* a direct and an indirect pathway *via* formation of salicylic aldehyde. At phenol conversion above 0.05%, anisole and *o*-cresol were the only reaction products. The two products do not interconvert. It is known from literature that in the presence of acid catalysts anisole may be an alkylating agent [41]. With the present MgO catalysts, however, anisole did not convert. At 450 °C, a small amount of phenol was formed from anisole decomposition because methylanisole was not observed. Thus, over MgO anisole is a stable compound.

Salicylic aldehyde is likely formed by the reaction between phenol and formaldehyde, the latter having formed by methanol dehydrogenation [41,42]. Salicylic aldehyde is a very reactive intermediate that can be recovered only under very unusual reaction conditions, i.e., low temperatures as well as extremely low contact times and phenol conversions (Fig. 1). At low temperatures, however, the dehydrogenation of methanol to formaldehyde is less favored [41]. The question arises, therefore, whether salicylic aldehyde is the reaction intermediate in the formation of *o*-cresol under reaction conditions leading to high phenol and methanol conversions. It should be noted that the reaction between phenol and formaldehyde should lead to the formation of salicylic alcohol as a first intermediate and not to the formation of salicylic aldehyde. In order to explore the proposed reaction pathway theoretical calculations and IR spectroscopic measurements were combined to understand surface structures and potential intermediates.

3.2. Sorption of phenol, o-cresol, salicylic alcohol, and salicylic aldehyde on MgO

Fig. 2 compiles the optimized models for the adsorption of phenol, *o*-cresol, salicylic alcohol, and salicylic aldehyde on three different sites of a $(MgO)_{12}$ cluster representing MgO surface sites. In order to account for the differences in the co-ordination of Mg and O, the sites for adsorption considered are those corresponding to the corner, step (edge), and terrace positions. Table 1 compiles the main molecular properties in the adsorbed state, i.e., adsorption energy, interatomic distances, and the COH angle at equilibrium. For comparison, the reference values for the corresponding isolated molecules are also given.

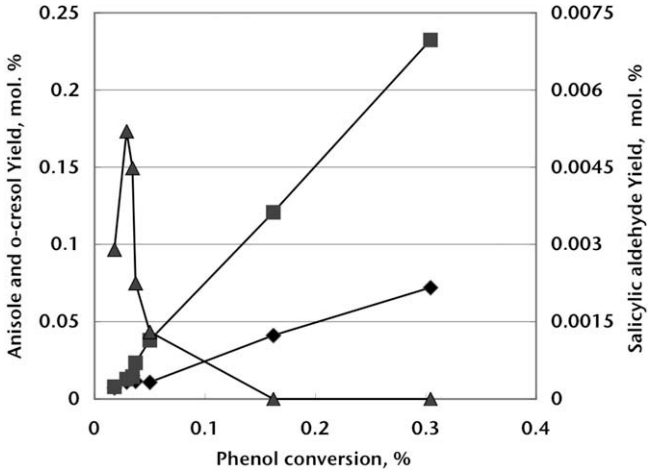

Fig. 1. Selectivity to products as function of phenol conversion in the reaction between phenol and methanol over low-surface-area MgO. Reaction conditions: *T* 300 °C; residence time range: 0.04–0.4 *s*; methanol-to-phenol molar feed ratio = 10/1. Symbols: anisole (♦), salicylic aldehyde (▲), and *o*-cresol (■).

The adsorption energies on the terrace site are in general weak, but are higher for step sites and the highest on corner sites, i.e., the values increase with decreasing co-ordination of the atom. With increasing strength of interaction the phenolic O–H bond length in the molecule increases causing a more pronounced distortion in the molecular geometry. For adsorption on terrace sites, the O–H group interacts associatively. Upon adsorption on co-ordinatively unsaturated sites the O–H group dissociates. It should be noted that adsorption of phenol on MgO is reported to lead to phenolate species and surface O–H groups [50]. The energetically most favored adsorption configuration is that one in which the adsorbed molecule adopts an orthogonal orientation with respect to the MgO surface. In agreement with the literature [7,9], we conclude that this orientation is caused by the repulsion of the aromatic ring by the electron-rich surface oxygen.

The IR spectra for sorptive molecules adsorbed over the different defective sites of MgO and for the corresponding gas-phase molecule were calculated. In the case of phenol (Fig. S2 of Supplementary material) the spectra of the adsorbed molecules are similar, the only relevant difference being the frequency of C–O stretching band at 1300 cm^{-1} when phenol is adsorbed in the corner position, but at considerably lower values for the step (1237 cm^{-1}) and the terrace (1241 cm^{-1}) positions, pointing out for differences in the C–O bond strength. The same is observed for *o*-cresol.

Experimental IR spectra were recorded after adsorption of the molecules on synthetic high-surface-area MgO; Fig. 3 compiles the difference IR spectra of phenol, *o*-cresol, salicylic alcohol, and salicylic aldehyde, at 250 °C. Attribution of bands to specific vibration modes was done by comparing experimental with calculated IR spectra, for adsorption at the corner site, which according to the computational study is the energetically preferred one. For example, Table S1 summarizes the experimental and calculated frequencies and the corresponding vibration modes for phenol adsorption.

In the case of spectrum recorded after phenol adsorption, a small negative band at 3740 cm^{-1} indicates that some phenol molecules interact with residual O–H groups on the MgO surface. Two small bands of perturbed O–H groups at 3705 and 3581 cm^{-1} are also observed. Between 3010 and 3070 cm^{-1} bands of stretching vibrations of C–H in the aromatic ring are observed, at 1602 cm^{-1} and at 1491 cm^{-1} the C–C ring vibrations, and at 1170 and at 1074 cm^{-1} the band of C–H bending. The band at 1300 and 1264 cm^{-1} are attributed to C–O stretching mode. As with phenol, in the case of *o*-cresol a small negative band is observed at 3740 cm^{-1}, together with two bands of perturbed O–H groups at 3713 and 3585 cm^{-1}. As for phenol, the adsorption at 250 °C leads to an alteration of vibration modes of phenolic OH in the 1200 cm^{-1} region, due to the dissociation of the hydroxyl group.

The difference IR spectrum for salicylic alcohol indicates adsorption on O–H groups (negative band at 3740 cm^{-1}) and shows perturbed O–H groups at 3701 and 3584 cm^{-1}. The bands between 2800 and 2950 cm^{-1} are attributed to C–H stretching of the hydroxymethyl group, while bands between 3000 and 3100 cm^{-1} are attributed to the C–H stretching vibrations of the aromatic ring. Band at 1449 cm^{-1} is attributed to the bending of the C–H in the hydroxymethyl group. At 1597 and 1538 cm^{-1} the aromatic C–C stretching vibrations and at 1281 cm^{-1} the

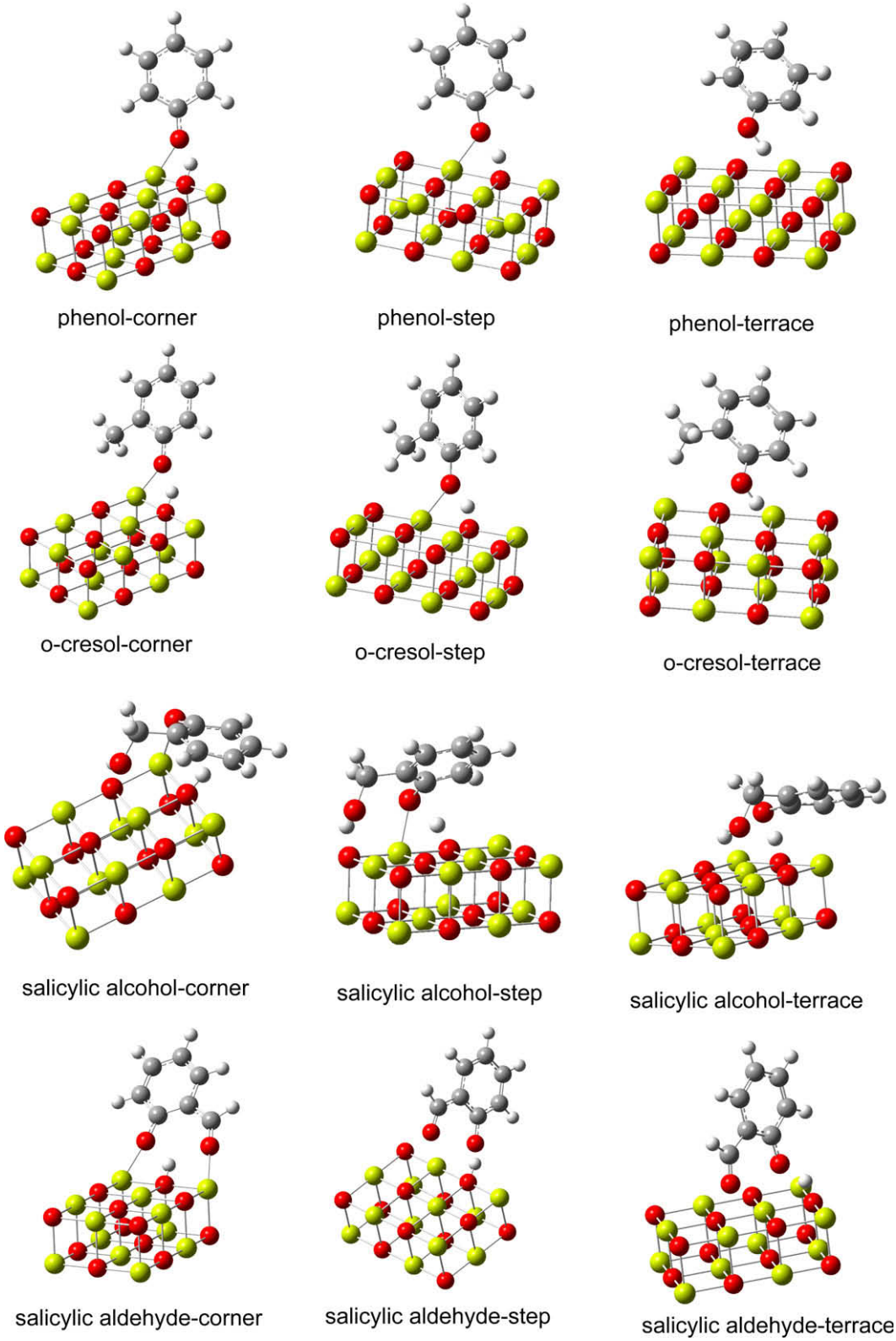

Fig. 2. Models of adsorption for (from top to bottom) phenol, *o*-cresol, salicylic alcohol, and salicylic aldehyde at the different sites of the $(MgO)_{12}$ cluster (from left to right): corner site, step site, and terrace site.

stretching of the bond between the O atom and the aromatic ring are observed. The band at 1153 cm^{-1} is assigned to the C–CH_2OH stretching vibration. The band at 1629 cm^{-1} in the spectrum of the adsorbed alcohol is tentatively attributed to a fraction of salicylic aldehyde formed upon adsorption (see below). The main difference between the experimental and the gas-phase spectrum

Table 1
Main molecular properties of phenolic reactants, intermediates, and products adsorbed on MgO surface: adsorption energy (E_{ads}), interatomic distances (d), and angle (Å) at equilibrium. In parenthesis are given the BSSE-corrected adsorption energies.

	Phenol-isolated	Phenol-corner	Phenol-step	Phenol-terrace
E_{ads} (kcal mol^{-1})		−43	−27 (−20)	−17 (−10)
d (Mg_{cry}–O_{mol}) (Å)		1.909	2.021	2.691
d (O_{cry}–H_{mol}) (Å)		1.001	1.055	1.647
d (O–H) (Å)	0.966	1.709	1.421	1.010
d (C–O) (Å)	1.389	1.342	1.346	1.363
A (CÔH) (°)	108.83	128.77	128.71	111.29
	o-Cresol-isolated	*o*-Cresol-corner	*o*-Cresol-step	*o*-Cresol-terrace
E_{ads} (kcal mol^{-1})		−40	−24 (−17)	−14 (−8)
d (Mg_{cry}–O_{mol}) (Å)		1.912	2.037	2.661
d (O_{cry}–H_{mol}) (Å)		1.000	1.070	1.646
d (O–H) (Å)	0.965	1.704	1.393	1.010
d (C–O) (Å)	1.370	1.340	1.349	1.366
A (CÔH) (°)	109.41	141.00	122.65	111.08
	Salicylic alcohol-isolated	Salicylic alcohol-corner	Salicylic alcohol-step	Salicylic alcohol-terrace
E_{ads} (kcal mol^{-1})		−54	−35 (−22)	−30 (−16)
d (Mg_{cry}–O_{mol}) (Å)		1.997	2.057	2.492
d (O_{cry}–H_{mol}) (Å)		0.972	1.037	1.053
d (O–H) (Å)	0.977	2.426	1.519	1.449
d (C–O) (Å)	1.361	1.315	1.346	1.316
A (CÔH) (°)	106.94	52.245	107.82	104.65
d (Mg_{cry}–O_{Alc}) (Å)		2.384	2.258	2.317
d (O_{cry}–H_{Alc}) (Å)		1.749	1.415	1.948
d (O–H_{Alc}) (Å)	0.966	0.996	1.051	0.981
d (CH_2–O_{Alc}) (Å)	1.444	1.439	1.431	1.441
	Salicylic aldehyde-isolated	Salicylic aldehyde-corner	Salicylic aldehyde-step	Salicylic aldehyde-terrace
E_{ads} (kcal mol^{-1})		−61	−25 (−17)	−4 (6)
d (Mg_{cry}–O_{mol}) (Å)		2.049	2.152	2.244
d (O_{cry}–H_{mol}) (Å)		0.974	1.007	1.031
d (O–H) (Å)	0.989	1.758	1.586	1.496
d (C–O) (Å)	1.339	1.295	1.306	1.308
A (CÔH) (°)	107.03	115.98	128.91	142.70
d (Mg_{cry}–O_{Ald}) (Å)		2.101	2.198	2.273
d (C=O_{Ald}) (Å)	1.235	1.253	1.241	1.225

(NIST library) concerns the C–O stretching vibration shifting from 1237 cm^{-1} (in the gas-phase spectrum) to 1291 cm^{-1} (in the experimental one).

For adsorbed salicylic aldehyde, bands between 3000 and 3090 cm^{-1} (attributed to the C–H stretching bands of the aromatic ring) as well as bands at 2876 and 2779 cm^{-1} (attributed the stretching of the C–H band of the aldehyde group) are observed; the latter one derives from the Fermi resonance [51]. The characteristic band of the aldehyde C=O stretching vibration appears at 1638 cm^{-1}. The strong shift to lower wavenumbers compared to the gas-phase spectrum (1680 cm^{-1}, NIST library) is due to the interaction of the carbonyl group with Mg^{2+} cations acting as Lewis acid sites. The bands at 1606 and 1535 cm^{-1} are attributed to the aromatic ring stretching vibrations, while the bands between 1409 and 1467 cm^{-1} to C–H bending vibrations. The band at 1333 cm^{-1} is attributed to C–O, being remarkably shifted with respect to the corresponding bands in *o*-cresol and salicylic alcohol spectra. The band at 1149 cm^{-1} corresponds to the vibration of C–CHO. According to the computational model, the salicylic aldehyde is deprotonated leading to an enhanced resonance effect and the consequent alteration of the vibrations of the carbonyl group. The stabilization of the aldehyde group by the basic O^{2-} and the Mg^{2+} cation is in agreement with the shift experimentally found for the carbonyl bond stretching. It is important to note that the aldehyde interacts with MgO at 250 °C but does not undergo any transformation such as the dismutation via the Tishchenko reaction [52]. This implies that salicylic aldehyde can be isolated as an intermediate in the reaction between phenol and methanol.

3.3. IR spectra of methanol under reaction conditions

Fig. 4 compares the difference spectra registered in the presence of flowing methanol at 250 °C over the high-surface-area MgO with the gas-phase spectrum of methanol. The shape and intensity of the bands indicate that some contribution of gas-phase methanol is present in the difference spectra. On the other side, the difference between the spectrum of methanol in the gas-phase and that of flowing methanol over MgO also show that bands due to surface structures can be discriminated from the overlaying gas-phase spectra.

An increase in the feed time led to an increase in the intensity for bands at 1009 (shoulder) and 1031 cm^{-1}; the same occurred for the most intense peak at 1061 cm^{-1}. Bands at 1116 and 1160 cm^{-1} are assigned to adsorbed methanol. The latter band is attributed to the rocking vibration of methyl group [36]. In this region, the bands due to vibrations of gas-phase methanol are easily recognized. Above 1300 cm^{-1}, bands at 1359, 1394, 1455, and 1584 cm^{-1} were observed. In the wavenumber region of C–H stretching bands characteristic of gas-phase methanol overlapped with bands attributed to adsorbed methanol. A broad band was observed between 3550 and 3730 cm^{-1}, together with a negative peak at 3747 cm^{-1} attributed to hydrogen bonding on MgOH groups.

One relevant aspect of this experiment is the asynchronous variation of the intensities during the reaction of methanol, especially in the region between 1200 and 1800 cm^{-1}. The relative intensities of bands at 1322, 1332, 1359, 1394, 1455, 1477, and 1584 cm^{-1} remained approximately constant. The bands with maxima at 1610

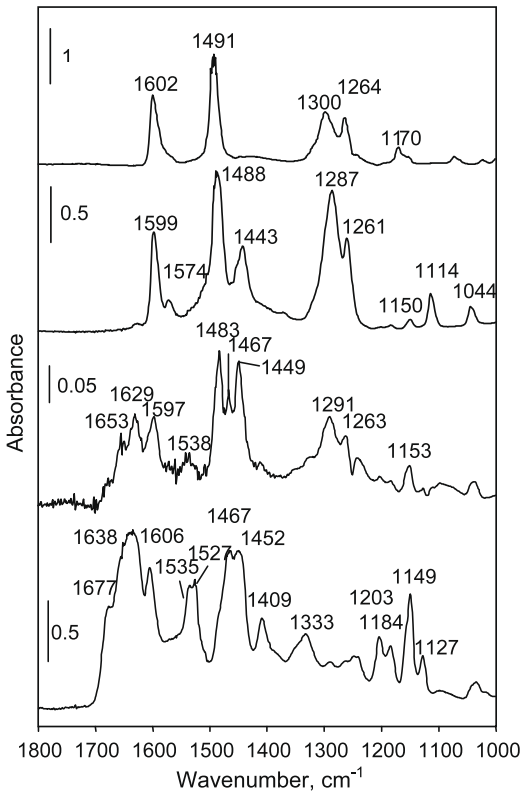

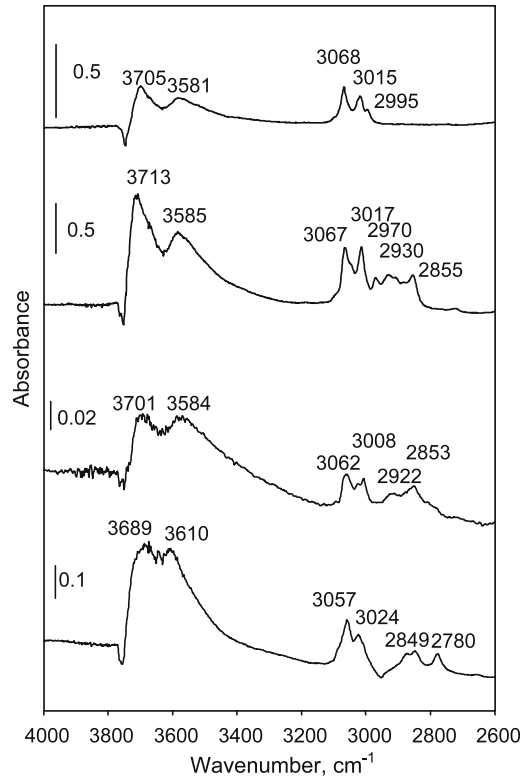

Fig. 3. Difference IR spectra of phenol (top spectrum), *o*-cresol (middle top spectrum), salicylic alcohol (middle bottom spectrum), and salicylic aldehyde (bottom spectrum) adsorbed over high-surface-area MgO.

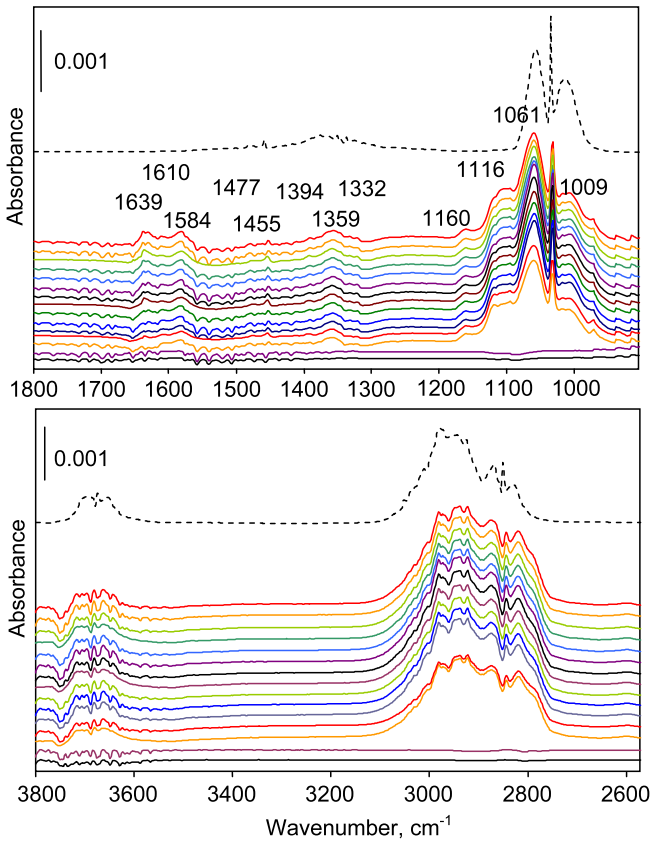

Fig. 4. Details of spectral regions from the spectra recorded by flowing methanol at 250 °C (dotted spectrum: gas-phase methanol) over the high-surface-area MgO. Spectra plotted at increasing times from bottom to top.

and 1639 cm^{-1} appeared only after some minutes after methanol was admitted and finally became more intense than the band centered at 1584 cm^{-1}. These bands are attributable to stretching vibrations of carbonates having different co-ordination [53]: ν_s COO– at 1322, 1359, and 1394 cm^{-1}, and ν_{as} COO– at 1639, 1610, and 1584 cm^{-1}, while the νCH_3 falls at 1332 cm^{-1}. The shoulder at 2790 cm^{-1} is likely due to the combined mode ν_s(COO–) + ν(CH). The band with maxima at 1610 and 1639 cm^{-1} (and the corresponding symmetric stretching vibrations) can be attributed to the formation of bidentate carbonates, while that one at 1584 cm^{-1} is related to the development of formate species (1584 ν_{as}, 1390 ν_s, 2790 νC–H) [54]. Therefore, the data indicate the initial formation of formates followed by the slower formation of carbonates.

Fig. 5 displays the spectra recorded at 450 °C. Under these conditions, the contribution of gas-phase methanol was lower than that at 250 °C. The band in the region between 1500 and 1700 cm^{-1} has maxima at 1612 and 1628 cm^{-1}, with shoulders at 1590 and 1560 cm^{-1}. The band is similar to that obtained by dosing CO_2 over MgO [55]. In contrast with what observed at 250 °C, there was no asynchronous variation of bands; this is likely due to the fact that the reaction having the higher activation energy was kinetically favored at the higher temperature. An evident phenomenon is the development of negative peaks in the hydroxyl zone at 3747 cm^{-1} and at 1540 cm^{-1} (νCOO–) in the carbonates zone; it is an evidence of the presence of a methanol decomposition phenomenon. At 2780 and 2750 cm^{-1} are the bands due to the stretching vibration of the aldehydic C–H bond.

3.4. IR Spectra during reaction of methanol and phenol

Fig. 6 reports the spectra recorded, while feeding methanol and phenol at 250 °C over the high-surface-area MgO, after subtraction of the MgO spectrum, and with the further subtraction of the

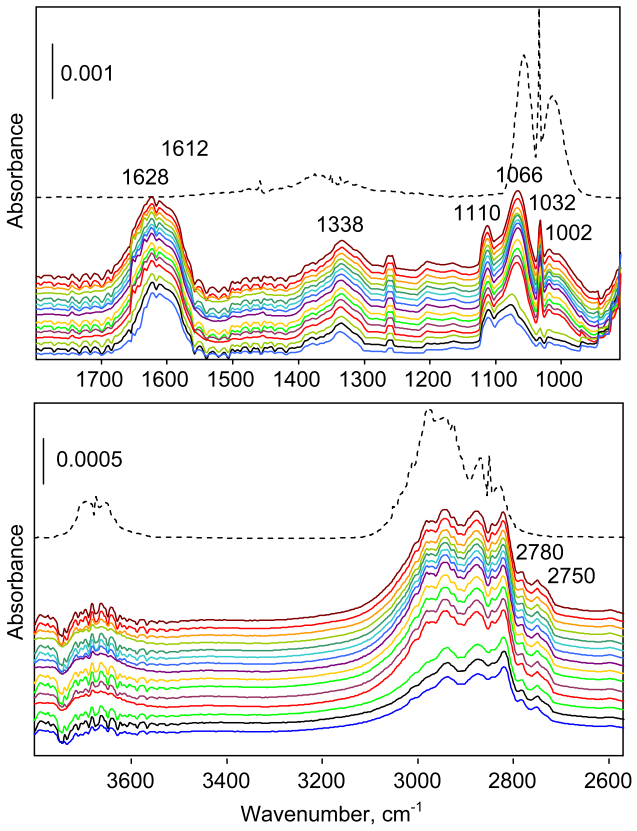

Fig. 5. Details of spectral regions from the spectra recorded by flowing methanol at 450 °C (dotted spectrum: gas-phase methanol) over the high-surface-area MgO. Spectra plotted at increasing times from bottom to top.

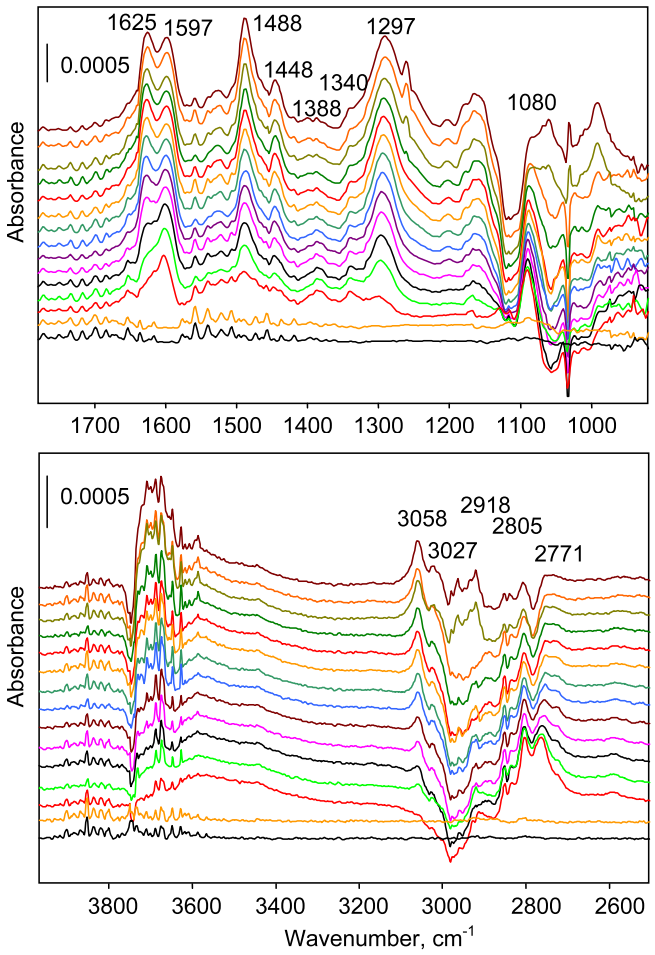

Fig. 6. Difference IR spectra of surface species while passing methanol and phenol over high-surface-area MgO and the IR spectra in the presence of methanol only (Fig. 4) at 250 °C. Spectra plotted at increasing times from bottom to top.

corresponding spectra obtained when only methanol was fed at the same time on stream (Fig. 4). This allows to minimize the interference of methanol (in the gas-phase and adsorbed state) and of its products of transformation. Clearly, this is valid only provided the reaction network of methanol transformation is the same both in the absence and in the presence of phenol. Indeed, the spectra obtained have negative bands, likely due to the fact that the corresponding products formed from methanol either did not form in the presence of phenol or readily reacted with the latter.

It is evident that the spectrum recorded after reaction includes not only the bands relative to adsorbed reactants, but also additional bands due to the reaction products. One important feature was the band at 1597 cm^{-1} that was present both in the spectrum recorded after reaction and in the spectra of reaction intermediates as well (Fig. 3). Also the band at 1488 cm^{-1} was present in all spectra, but not in that of adsorbed salicylic alcohol. The band at 1080 cm^{-1} is likely to be attributed to methanol. An intense peak at 1625 cm^{-1} was also present in the spectrum of adsorbed salicylic aldehyde (but it cannot be excluded to be due to a formate species). In the spectral region between 3200 and 2600 cm^{-1}, the band at 2805 cm^{-1} can be attributed to methanol or to a product of its transformation, while bands between 3058 and 3027 cm^{-1} are due to aromatic C–H vibrations.

The main time-dependent features of the spectra include (i) the progressive increase in the intensity of band at 1448 cm^{-1} attributed to the CH_3 bending vibration in *o*-cresol, (ii) the concomitant decrease in the intensity of the aldehydic C–H stretching band between 2700 and 2800 cm^{-1}, and (iii) the increase in the band at 1625 cm^{-1}.

The spectra reported in Fig. 6 show the progressive increase in the intensity for bands at 1297, 1340, 1388, 1448, 1488, 1625, 3027, and 3058 cm^{-1}, and the decrease in the intensity for bands at 2918, 2805, and 2771 cm^{-1}. This indicates that at short times on stream the relative concentration of the adsorbed species changes remarkably. At first, the band at 1448 cm^{-1} is in line with the rapid formation and adsorption of *o*-cresol. With time on stream, an aromatic compound with a C=O group (1625 cm^{-1}, i.e., salicylic aldehyde) increases in concentration. Both products seem to be stable under the reaction conditions probed, and evidences for the interconversion are not observable in the *in situ* IR spectra.

3.5. The reactivity of salicylic alcohol

Spectroscopic measurements and catalytic tests suggest that one key intermediate of the reaction is salicylic alcohol. In order to understand the possible elementary steps for the transformation of salicylic alcohol into *o*-cresol, we performed reactivity tests by feeding either a salicylic alcohol/water solution or a salicylic alcohol/formalin aqueous solution, both vaporized in a N_2 stream. Table 2 summarizes the results obtained at 300 °C.

In both cases, there was a total conversion of salicylic alcohol; this explains why this compound was not isolated as an intermediate in phenol methylation even at a very low contact time (Fig. 1). In the absence of formaldehyde, salicylic alcohol produced phenol and *o*-cresol in an almost equimolar amount. The C balance, however, was close to 80–85%, highlighting the formation of heavy

Table 2
Reactivity of salicylic alcohol over MgO at 300 °C.

Product	Selectivity (%)	
	Feed: salicylic alcohol in water	Feed: salicylic alcohol in aqueous formalin
Phenol	45	10
o-Cresol	55	35
2,6-Xylenol	0	24
Salicylic aldehyde	0	3
2-Hydroxy-3-methylbenzaldehyde	0	1
Toluene	0	1
2,4,6-Trimethylphenol	0	13
4H-benzo[1,3]dioxine	0	13

by-products; the latter were identified as di-aryl compounds, formed either by condensation of the hydroxymethyl groups of two salicylic alcohol molecules or the ring-alkylation of one salicylic alcohol molecule onto a second one. It is worthy of note that in the absence of catalyst still there was a total conversion of salicylic alcohol, and the same products obtained in the presence of MgO were also obtained, but with the predominance of *o*-cresol, while salicylic aldehyde formed in an amount equivalent to phenol. At 200 °C, both in the presence and in the absence of MgO, the total salicylic alcohol fed was converted to these heavy by-products. It is apparent that in the presence of a relatively high partial pressure of salicylic alcohol, the alcohol reacts very quickly with another molecule of alcohol, both in the presence and in the absence of catalysts, yielding di-aryl compounds, which possibly further decompose according to the stoichiometry:

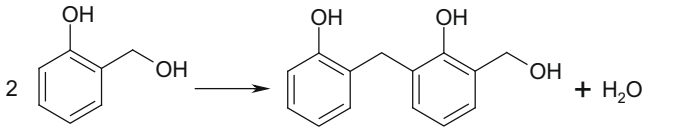

(1)

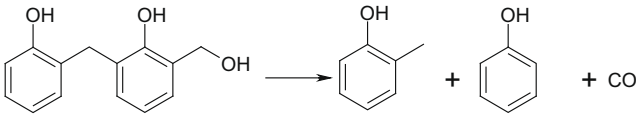

(2)

Heavy compounds may also form by the MgO-catalyzed condensation reaction of two adsorbed molecules of salicylic aldehyde, the latter having been formed by alcohol dehydrogenation. Moreover, phenol may also form by direct decomposition of salicylic alcohol:

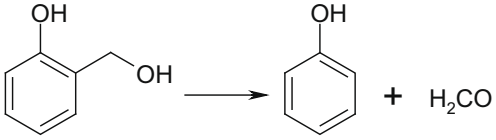

(3)

However, the formation of CO was very low, thus suggesting that a direct disproportion is likely the dominant mechanism for *o*-cresol formation from salicylic alcohol (reaction (4)), even though in the presence of MgO, the salicylic aldehyde formed remains strongly bound to the catalyst surface. Indeed, the spent catalyst was brown, thus confirming the accumulation of heavy compounds on its surface during reaction.

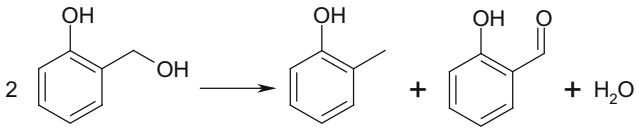

(4)

Tests made with salicylic alcohol and formalin yielded several compounds (Table 2); the prevailing ones were *o*-cresol, 2,6-xylenol, and 2,4,6-trimethylphenol, also with the presence of non-negligible amounts of phenol and 4H-benzo[1,3]dioxine. The mono-, di-, and tri-methylated phenols form by a reaction of phenol and *o*-cresol (the main compounds formed in the absence of formalin) with formaldehyde; the absence of the corresponding hydroxymethylated intermediates confirms that the latter are highly reactive. The dioxine forms by O-hydroxymethylation on the two hydroxy groups of salicylic alcohol, with the formation of a cyclic and relatively stable intermediate. The non-cyclic, less stable compound is the 2-hydroxy-3-methylbenzaldehyde, which formed in much smaller amount.

Among the light compounds, we noted the very significant formation of CO_2, with only traces of CO, and no formation of either methane or hydrogen. The absence of H_2 makes it possible to rule out reactions involving H_2O as the reactant (e.g., WGS of CO), and a Cannizzaro-like disproportion of formaldehyde leading to methanol (that was also not formed in the reaction; the small amount of methanol detected was that originally present in the formalin solution) and formic acid; in fact, the decomposition of the acid would lead either to CO_2 and H_2, or to H_2O and CO. Also, the absence of methane makes it possible to rule out a Tishchenko-like dimerization of formaldehyde to methylformate as well as its decomposition into CO_2 and CH_4. Therefore, the formation of CO_2 was most likely due to the Oppenauer-type oxidation:

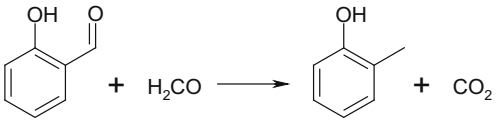

(5)

When the same reaction was carried out without the MgO catalyst, the predominant product was 4H-benzo[1,3]dioxine, with around 60% selectivity. *o*-Cresol also formed, but there were no di- and tri-methylated compounds. Therefore, at the conditions used (*T* 300 °C) the catalyst is essential for the C-hydroxymethylation reaction, but it is not necessary for the O-hydroxymethylation of salicylic alcohol, and the redox reaction between salicylic aldehyde and formaldehyde.

An experiment done by feeding salicylic aldehyde with formalin at 350 °C confirmed that the reaction (5) might be the one possible pathway for *o*-cresol formation. In fact, salicylic aldehyde gave almost total (98%) conversion to *o*-cresol (selectivity 30%) and 2,6-xylenol (selectivity 70%).

4. Discussion

4.1. The interaction of reactants and products with MgO

The interaction of methanol with MgO (as model oxide for basic oxides) has been studied by several authors [56–61] and it is well established that MgO catalyzes the dehydrogenation of methanol [62]. Chemisorption occurs via heterolytic dissociation [58] involving the formation of hydroxyl groups and CH_3O^- anions [63]. Further abstraction of H^- by an accessible Mg^{2+} cation or a carbonaceous residue completes the step. Formation of surface formate

species may occur through nucleophilic interaction of an adjacent oxygen atom with the carbon of the methylene group. Alternatively two sorbed formaldehyde molecules may disproportionate (via a nucleophilic attack) to formate and a methoxy species [60,64]. Formate may decompose to CO and H_2. Alternatively, adsorbed methoxy and formate species may yield methylformate (Tishchenko reaction) which is able to decompose at high temperatures to methane and CO_2 [65].

The present data show that already at 250 °C the interaction of methanol with the clean catalytic surface generates formate and carbonate species, giving unequivocal evidence for the dehydrogenation of methanol and of the strong interaction of the resulting products with the basic surface. At high temperature the extent of methanol decomposition was relevant indicating that the formaldehyde generated is very reactive and is rapidly transformed to light compounds, i.e., CO, CH_4, and CO_2.

In line with the earlier reports [23,50,66,67] the present data show that the adsorption of phenol and phenol analogs (*o*-cresol, salicylic alcohol, and salicylic aldehyde) on highly co-ordinatively unsaturated sites (corner sites) is energetically favorable. In this case, the interaction between MgO and the adsorbate is very strong and leads to the dissociation of the sorbate at room temperature.

4.2. The reaction between adsorbed reactants

In the literature, the mechanism of reaction between phenol and methanol catalyzed by basic oxides is believed to occur by a direct electrophilic substitution on the aromatic ring with only few papers considering a possible role of formaldehyde. Palomares et al. [39,40] demonstrated that in the base-catalyzed side-chain methylation of toluene to styrene, it is important that (i) methanol needs to be dehydrogenated to formaldehyde forming a strongly positively polarized C atom (through the interaction between the carbonyl and the metal cation) and (ii) the methyl group of toluene needs to interact with the basic oxygen atoms to form a partial negative charge on the C atom. In consequence, an aldol-type C–C bond formation may occur followed by dehydration and the formation of the C=C moiety. The limiting factor in this chemistry is the low stability of the intermediately formed formaldehyde which would lead to partial decomposition at the reaction temperatures required for side-chain alkylation.

The question arises if intermediately formed formaldehyde would also play an important role in the *C*-alkylation of phenol over basic catalysts. Due to the higher intrinsic reactivity of the aromatic ring, methylation may occur under milder reaction conditions and with catalysts having lower basic strength than for the side-chain alkylation of toluene.

Indirect evidence for such chemistry has been reported in the literature. Using IR spectroscopy Mathew et al. [23] studied the development of formaldehyde, dioxymethylene, and formate species from methanol on Cu/Co/Fe/O catalysts (decomposition of the products above 300 °C), but also reported that due to the competition of phenol for adsorption on the sites responsible for methanol oxidation, decomposition did not occur in the presence of both compounds. Padmasri et al. [27] also speculated that in the reaction between phenol and isobutanol on MgO and on calcined hydrotalcites, the alkoxy species might dehydrogenate forming an adsorbed isobutyraldehyde intermediate. The latter then was reported to react with phenol to yield either *o*-butenylphenol, after dehydration of the intermediate alcohol, or 2-butenylphenol.

In recent contributions [41,42] it was shown by us that under conditions favoring methanol dehydrogenation, formaldehyde is the true reacting species with the phenolate yielding *o*-cresol and 2,6-xylenol. The products obtained at low temperatures and conventional contact times are anisole and *o*-cresol, the latter dominating between 300 and 450 °C. It is important to note that the lower the temperature is, i.e., the lower the degree of dehydrogenation of methanol, the more significant the formation of anisole becomes. We also found that reacting phenol with formalin yielded the same product distribution as that obtained by reacting phenol with methanol.

The catalytic tests demonstrate that at moderate temperature (i.e., 300 °C) salicylic aldehyde is a primary reaction product (next to *o*-cresol and anisole) which can be isolated only at very low phenol conversions (low contact time). As it is seen as product accumulating also with higher time on stream (see Fig. 6) we conclude that when more products and reactants are sorbed at the surface, salicylic aldehyde reacts preferentially with surface species to *o*-cresol. Under conditions of low surface coverage, salicylic aldehyde is not further converted to consecutive products because the low concentration of adsorbed methanol and formaldehyde makes the secondary reaction less likely. When the concentration of molecules at the adsorbed state increases, salicylic aldehyde is rapidly transformed to *o*-cresol. We speculate at present that the salicylic aldehyde transformation may occur in bimolecular disproportionation-like reaction (intermolecular H-transfer) from adsorbed methanol, formaldehyde, or another functionalized aromatic compound.

The reaction between an activated aromatic molecule and formaldehyde is also known as hydroxymethylation, and leads to the formation of salicylic alcohol in the case of phenol. This reaction occurs in the liquid phase at moderate temperatures, and is catalyzed by acidic and basic catalysts [68,69]. The IR spectra of adsorbed salicylic alcohol (see characteristic bands at 1653 and 1629 cm^{-1} in Fig. 3) indicate that at least a significant fraction is rapidly transformed to salicylic aldehyde.

4.3. The mechanism of transformation of salicylic alcohol into o-cresol

Reactivity tests made by feeding salicylic alcohol showed that this compound, the very first intermediate in the C-hydroxymethylation of phenol by formaldehyde, is very reactive and is rapidly transformed into either heavy di-aryl compounds or mono-aryl phenolic compounds. The formation of heavy products (a reaction occurring even in the absence of catalyst) is significant when salicylic alcohol is directly fed into the reactor, but is likely less important during the reaction of phenol methylation.

The transformation of alcohol into salicylic aldehyde, a primary product of the reaction (Fig. 1), may occur *via* either direct dehydrogenation, or disproportionation (reaction (4)), which would explain the experimental evidence of both phenolic compounds being primary products (Fig. 1), as well as the substantial absence of light compounds (CO, CO_2, H_2) in tests made by feeding salicylic alcohol.

Finally, the consecutive transformation of salicylic aldehyde to yield *o*-cresol occurs by an Oppenauer-type oxidation which explains the formation of CO_2 (reaction (5)).

A similar reaction may occur between salicylic alcohol and formaldehyde to yield *o*-cresol as one primary reaction product:

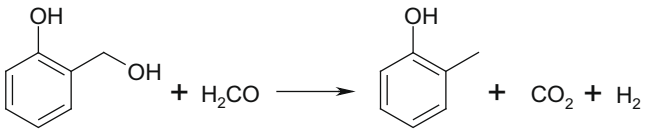

(6)

This reaction may prevail over that involving two molecules of salicylic alcohol (reactions (1) and (2)) under conditions of low surface concentration of the adsorbed intermediates, that is, under the conditions normally used for phenol methylation.

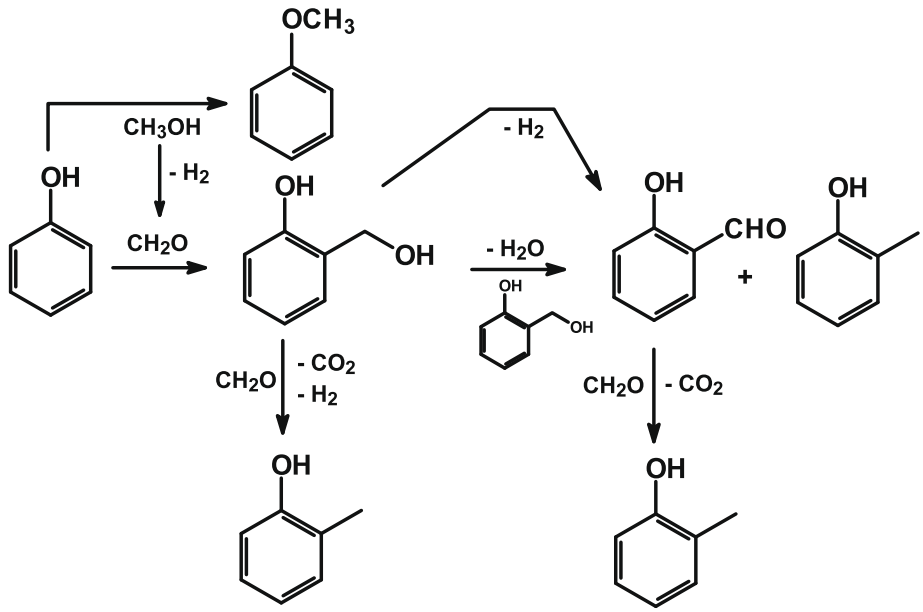

Fig. 7. Overall reaction scheme of phenol methylation with methanol catalyzed by MgO.

Tests made without the catalyst showed that under the conditions used, the catalyst is essential for the C-hydroxymethylation reaction (phenol to salicylic alcohol), but it may not be necessary for the disproportion of salicylic alcohol to *o*-cresol and salicylic aldehyde, and the consecutive reaction between salicylic aldehyde and formaldehyde to yield *o*-cresol.

It is worth noting that in the reaction between phenol and methanol, salicylic aldehyde can be isolated only when extremely low contact times are used (Fig. 1), i.e., under conditions at which the surface coverage by adsorbed species is very low. When, on the contrary, reaction conditions are used that may favor the accumulation of adsorbed intermediates on the catalyst surface, e.g., by feeding salicylic alcohol and by using low reaction temperatures, the formation of heavy compounds is kinetically preferred. Finally, when reacting phenol and methanol at normal reaction conditions the concentration of adsorbed salicylic alcohol and aldehyde is very low, and the two compounds readily react with methanol and formaldehyde to yield *o*-cresol.

The third primary product, anisole, is only observed at low temperatures. It is formed by direct reaction between activated methanol and phenol with water as the leaving group. Because at high temperature, i.e., under conditions at which methanol dehydrogenation occurs with feasible rates, the only reaction products are *o*-cresol and 2,6-xylenol, we conclude that the reaction occurs in a concerted mechanism using the polarization of the phenol OH and methanol C–O bond. Because we compare the selectivity at different temperature for two different routes, if the activation energies for both are far different, the selectivity will be different. It seems, the anisole formation with very low activation energy and at low temperature, it is the favorite product. Alternatively it could be speculated that anisole is formed by a reaction between phenolate and methylformate (formed by dimerization of HCHO). At higher temperature, methylformate readily decomposes to, e.g., CH_4 and CO_2.

5. Conclusions

The combination of catalytic tests, IR spectroscopy of adsorbed reactants, products, and possible intermediates together with a computational study as well as *in situ* IR spectra during reaction allows for a full description of the reaction network in the methylation of phenol (see Fig. 7).

The nature of the products generated by methanol interacting with the catalyst is a function of the reaction conditions, and it affects the primary products obtained in phenol methylation. Under conditions at which the extent of methanol dehydrogenation is low, i.e., low temperature, the main primary products of reaction are anisole and *o*-cresol. Under conditions more favorable for methanol dehydrogenation, anisole is no longer formed, and *o*-cresol becomes the only reaction product. 2,6-Xylenol forms in significant concentrations above 350 °C and for high phenol conversion. The adsorption of phenol on MgO generates a phenolate species, and the energetically preferred mode of adsorption is on the corner site of MgO, with an almost orthogonal orientation of the aromatic ring with respect to the catalyst surface. The adsorption of *o*-cresol and of the reaction intermediates, salicylic alcohol, and salicylic aldehyde at the corner site of MgO is also energetically favored. In all cases, the adsorbed molecules dissociate forming a phenolate-like species and a hydroxyl group.

The reaction between adsorbed phenolate and formaldehyde generates salicylic alcohol via hydroxymethylation, which is rapidly transformed to salicylic aldehyde. At low temperature and for very low conversions and short residence time, salicylic aldehyde is one of the primary reaction products. However, the aldehyde is very rapidly transformed into *o*-cresol, and is not detectable for phenol conversion higher than 0.05%. Below 300 °C anisole and *o*-cresol are formed, the latter being formed *via* either direct reduction of salicylic alcohol by formaldehyde, or the bimolecular disproportion of salicylic alcohol to *o*-cresol and salicylic aldehyde.

In situ spectroscopy shows salicylic aldehyde to be the reaction intermediate in *o*-cresol formation. The latter is observed during the initial accumulation of adsorbed species on the catalyst surface, i.e., while a low surface coverage prevails. It is not observed under steady conditions, i.e., when the catalyst surface is fully covered, in line with the fact that salicylic aldehyde is only observed at extremely low conversions.

Overall the results demonstrate that subtle tailoring of the base properties allows to use methanol in a dual role as alkylating agent and as reducing agent of the alcohol/aldehyde group created. While this is important for the selective alkylation of phenols, the insight into the reaction may even be more important for the defunctionalization of substituted phenols potentially available at large scale from deconstructed lignin.

Acknowledgments

This work has been conducted in the framework of Network of Excellence IDECAT (FP6 of the EU). INSTM is acknowledged for the Grant of SP and LM.

Appendix A. Supplementary material

Supplementary data associated with this article can be found, in the online version, at doi:10.1016/j.jcat.2009.11.019.

References

[1] H. Hattori, Chem. Rev. 95 (1995) 537.
[2] Y. Ono, T. Baba, Catal. Today 38 (1997) 321.
[3] R.J. Davis, J. Catal. 216 (2003) 396.
[4] Y. Ono, J. Catal. 216 (2003) 406.
[5] A. Cimino, F.S. Stone, Adv. Catal. 47 (2002) 141.
[6] M. Barteau, Chem. Rev. 96 (1996) 1413.
[7] K. Tanabe, T. Nishizaki, in: G.C. Bond et al. (Eds.), Proceedings of Sixth ICC, The Chemical Society, London, 1977, p. 863.
[8] S. Sato, K. Koizumi, F. Nozaki, Appl. Catal. A 133 (1995) L7.
[9] K. Tanabe, H. Hattori, T. Sumiyoshi, K. Tamaru, T. Kondo, J. Catal. 53 (1978) 1.
[10] R. Bal, B.B. Tope, S. Sivasanker, J. Mol. Catal. A 181 (2002) 161.
[11] K.T. Li, I. Wang, K.R. Chang, Ind. Eng. Chem. Res. 32 (1993) 1007.
[12] V. Durgakumari, S. Narayanan, J. Mol. Catal. 65 (1991) 385.
[13] K. Tanabe, K. Shimazu, H. Hattori, K. Shimazu, J. Catal. 57 (1979) 35.
[14] T. Kotanigawa, K. Shimokawa, Bull. Chem. Soc. Jpn. 47 (1974) 950 and 1535.
[15] H. Grabowska, W. Kaczmarczyk, J. Wrzyszcz, Appl. Catal. 47 (1989) 351.
[16] S. Velu, C.S. Swamy, Appl. Catal. A 145 (1996) 141.
[17] V.V. Rao, K.V.R. Chary, V. Durgakumari, S. Narayanan, Appl. Catal. 61 (1990) 89.
[18] S. Karuppannasamy, K. Narayanan, C.N. Pillai, J. Catal. 66 (1980) 281.
[19] H. Grabowska, W. Mista, J. Trawczynski, J. Wrzyszcz, M. Zawadzki, Appl. Catal. A 220 (2001) 207.
[20] K. Sreekumar, S. Sugunan, Appl. Catal. A 230 (2002) 245.
[21] T. Mathew, N.R. Shiju, K. Sreekumar, B.S. Rao, C.S. Gopinath, J. Catal. 210 (2002) 405.
[22] T. Mathew, S. Shylesh, B.M. Devassy, C.V.V. Satyanarayana, B.S. Rao, C.S. Gopinath, Appl. Catal. A 261 (2004) 292.
[23] T. Mathew, M. Vijayaraj, S. Pai, B.B. Tope, S.G. Hegde, B.S. Rao, C.S. Gopinath, J. Catal. 227 (2004) 175.
[24] S. Sato, K. Koizumi, F. Nozaki, J. Catal. 178 (1998) 264.
[25] S. Velu, C.S. Swamy, Appl. Catal. A 119 (1994) 241.
[26] S. Velu, C.S. Swamy, Appl. Catal. A 162 (1997) 81.
[27] A.H. Padmasri, A. Venugopal, V. Durgakumari, K.S. Rama Rao, P. Kanta Rao, J. Mol. Catal. A 188 (2002) 255.
[28] S. Sato, R. Takahashi, T. Sodesawa, K. Matsumoto, Y. Kamimura, J. Catal. 184 (1999) 180.
[29] T.M. Jyothi, T. Raja, M.B. Talawar, B.S. Rao, Appl. Catal. A 211 (2001) 41.
[30] M. Bolognini, F. Cavani, D. Scagliarini, C. Flego, C. Perego, M. Saba, Catal. Today 75 (2002) 103.
[31] F. Cavani, C. Felloni, D. Scagliarini, A. Tubertini, C. Flego, C. Perego, Stud. Surf. Sci. Catal. 143 (2002) 953.
[32] M. Bolognini, F. Cavani, D. Scagliarini, C. Flego, C. Perego, M. Saba, Micropor. Mesopor. Mater. 66 (2003) 77.
[33] F. Cavani, L. Maselli, D. Scagliarini, C. Flego, C. Perego, Stud. Surf. Sci. Catal. 155 (2005) 167.
[34] US Patent 4,933,509, 1989, assigned to General Electric.
[35] P.D. Chantal, S. Kaliaguine, J.L. Grandmaison, Appl. Catal. 18 (1985) 133.
[36] M. Bregolato, V. Bolis, C. Busco, P. Ugliengo, S. Bordiga, F. Cavani, N. Ballarini, L. Maselli, S. Passeri, I. Rossetti, L. Forni, J. Catal. 245 (2007) 283.
[37] R. Pierantozzi, A.F. Nordquist, Appl. Catal. 21 (1986) 263.
[38] S.T. King, J.M. Garces, J. Catal. 104 (1987) 59.
[39] A.E. Palomares, G. Eder-Mirth, J.A. Lercher, J. Catal. 168 (1997) 442.
[40] A.E. Palomares, G. Eder-Mirth, M. Rep, J.A. Lercher, J. Catal. 180 (1998) 56.
[41] N. Ballarini, F. Cavani, L. Maselli, A. Montaletti, S. Passeri, D. Scagliarini, C. Flego, C. Perego, J. Catal. 251 (2007) 423.
[42] N. Ballarini, F. Cavani, L. Maselli, S. Passeri, S. Rovinetti, J. Catal. 256 (2008) 215.
[43] S. Sasaki, K. Fujino, Y. Takeuchi, Proc. Jpn. Acad. 55 (1979) 43.
[44] E.A. Colbourn, J. Kendrick, C. Mackrodt, Surf. Sci. 126 (1983) 350.
[45] M.W. Wong, Chem. Phys. Lett. 256 (1996) 391.
[46] M.J. Frisch et al., Gaussian Inc., Wallingford CT, Gaussian 03, Revision C.02, 2004.
[47] R. Dennington II, T. Keith, J. Millam, K. Eppinnett, W.L. Hovell, R. Gilliland, GaussView, Version 3.09, Semichem Inc., Shawnee Mission, KS, 2003.
[48] G. Mirth, J.A. Lercher, J. Catal. 132 (1991) 244.
[49] G. Mirth, J.A. Lercher, J. Catal. 147 (1994) 199.
[50] R.N. Spitz, J.E. Barton, M.A. Barteau, R.H. Staley, A.W. Sleight, J. Phys. Chem. B 90 (1986) 4067.
[51] D.F. Eggers Jr., W.E. Lingren, Anal. Chem. 28 (1956) 1328.
[52] K. Tanabe, K. Saito, J. Catal. 35 (1974) 247.
[53] Y. Fukuda, K. Tanabe, Bull. Chem. Soc. Jpn. 46 (1973) 1616.
[54] G. Busca, J. Lamette, J.-C. Lavalley, V. Lorenzelli, J. Am. Chem. Soc. 109 (1987) 5197.
[55] J.V. Evans, T.L. Whateley, Trans. Faraday Soc. 63 (1967) 2769.
[56] G. Busca, Catal. Today 27 (1996) 457.
[57] J.C. Lavalley, Catal. Today 27 (1996) 377.
[58] J. Günster, G. Liu, J. Stultz, S. Krischok, D.W. Goodman, J. Phys. Chem. 104 (2000) 5738.
[59] C. Di Valentin, A. Del Vitto, G. Pacchioni, S. Abbet, A.S. Wörz, U. Heiz, J. Phys. Chem. B 106 (2002) 11961.
[60] X.D. Peng, M.A. Barteau, Langmuir 5 (1989) 1051.
[61] L.J. Burcham, L.E. Briand, I.E. Wachs, Langmuir 17 (2001) 6164.
[62] P. Mars, J.J. Scholten, P. Zwietering, Adv. Catal. 14 (1963) 35.
[63] M. Ziolek, J. Kujawa, O. Saur, J.C. Lavalley, J. Phys. Chem. 97 (1992) 9761.
[64] N.D. Lazo, D.K. Murray, M.L. Kieke, J.H. Haw, J. Am. Chem. Soc. 114 (1992) 8552.
[65] T. Mori, S. Hoshino, A. Neramittagapong, J. Kubo, Y. Morikawa, Chem. Lett. (2002) 390.
[66] D.R. Taylor, K.H. Ludlum, J. Phys. Chem. 76 (20) (1972) 2882.
[67] H. Hattori, K. Shimazu, N. Yoshii, K. Tanabe, Bull. Chem. Soc. Jpn. 49 (1976) 969.
[68] J. Lecomte, A. Finiels, P. Geneste, C. Moreau, Appl. Catal. A 168 (1998) 235.
[69] M. Ardizzi, F. Cavani, L. Dal Pozzo, L. Maselli, R. Mezzogori, Stud. Surf. Sci. Catal. 158 (2005) 1953.